Stefan Martens
Walter Mack
Infineon Technologies AG,
93049 Regensburg, Germany

Frédéric Courtade
Philippe Perdu
Centre National d'Etudes Spatiales, CNES,
31401 Toulouse, France

Juergen Wilde
Department of Microsystems Engineering (IMTEK),
Laboratory for Assembly and Packaging,
University of Freiburg,
79110 Freiburg, Germany

Friedemann Voelklein
Institute of Microtechnologies, IMtech,
University of Applied Sciences Wiesbaden,
65197 Wiesbaden, Germany

Laser-Based Target Preparation in 3D Integrated Electronic Packages

The trend toward 3D integration in electronic packaging requires that failure analysis procedures and target preparation methods are adapted from conventional discrete packages to these emerging packaging technologies. This paper addresses the feasibility of laser-based target preparation in 3D integrated devices, especially stacked-die packages. Various laser technologies such as ultrashort-pulse lasers, excimer lasers, and diode-pumped solid-state (DPSS) lasers with different wavelengths and pulse durations were evaluated. In particular, it was found that ultrashort-pulse lasers with pulse durations in the femtosecond range were not suitable for ablation of the molding compound (MC). Picosecond lasers were applicable with certain constraints. It was found that for MCs with high filler content, DPSS lasers with pulse durations in the nanosecond range were the best choice. For the removal of stacked silicon dies, the laser wavelength was the most important factor in artifact-free thinning. Laser cross sections through several silicon dies with remarkably small heat-affected zones were also demonstrated. The distinct removal of the MC, silicon dies, and metal interconnected with a single laser source offers new opportunities for laser-based target preparation in 3D integrated electronic packaging devices. [DOI: 10.1115/1.3144157]

1 Introduction

One of the major trends in electronic packaging is 3D integration. 3D integrated system-in packages (SiPs) are smaller, lighter, and thinner, and have improved interchip signals and power distribution. Moreover, SiP technology allows various electronic functions to be integrated flexibly within a single component. For example, stacked packages have become extremely important as combinations of memory and logic devices [1].

Reliability is one of the key prerequisites for the further success of SiPs compared with conventional packaging and interconnecting technologies. To improve the reliability of SiPs, diagnostic tools and failure analysis procedures must be adapted to the emerging SiP technology [2].

The removal of the molding compound (MC) for failure analysis is a standard process for semiconductors manufacturers who need visual access, and also have to perform mechanical measurements of wirebond pull and shear forces after reliability testing or in failure localization. Nondestructive magnetic, acoustic, and thermographic methods are insufficient because of the decrease in resolution caused by the MC.

Several years ago, chemical decapsulation and reactive ion etching (RIE) were mainly used for MC removal. Wet chemical processes were well established and optimized over many years [3], but nevertheless limited by corrosion of the chip metallization due to etch attack, damage to Cu wire bonds, overetching of leadframe platings, or MC that can be removed only by hot sulphuric acid [4].

Reactive ion etching is limited in two ways. Unless complex masks are used, RIE removes a complete package layer. Also, RIE systems are not capable of penetrating planar metal layers without the presence of hazardous gases such as chlorine, making investigations under such layers very difficult [5].

The laser ablation process for MC removal was developed for discrete packages [6–8]. However, it is not possible to ablate the MC completely without damaging the passivation or melting the metallization. A summary and overview of the state-of-the-art in laser-assisted decapsulation of MC-encapsulated devices by infrared diode-pumped solid-state (DPSS) lasers is given by Krueger et al. [4].

Because there are problems with pure chemical wet etching and with pure laser decapsulation, combining both methods is the current state-of-the-art. The MC is removed by laser except for the material remaining several micrometers above the die surface. The laser ablation process is stopped after the appearance of the bond wire loops. This is monitored by in situ video inspection. The remaining MC is removed within seconds by hot nitric acid or sulphuric acid or a mixture of both, depending on the prevalent metals on the chip surface.

Figure 1 shows the typical dimensions of a stacked-die package. The active integrated circuit (IC) structures of die 1 are covered by a silicon spacer, two more active dies (2 and 3), and the MC encapsulation. The MC is usually an epoxy matrix with a high content of silica filler particles in order to reduce thermal expansion. The chips are mounted with either 0.025 mm die attach (DA) tape or DA glue. The active IC structure consists of several oxide and nitride layers, as well as copper and aluminum metal layers.

Laser ablation of the silicon dies is not feasible with the infrared DPSS lasers that are usually used for MC removal. State-of-the-art for target preparation of these packages is mechanical cross-sectioning by coplanar grinding, or alternatively by high-precision milling machines.

There is a lot of published literature describing laser ablation of various materials, but most of the studies focus on ablation of one or two distinct materials with one specific laser source. It was not

Contributed by the Electrical and Electronic Packaging Division of ASME for publication in the JOURNAL OF ELECTRONIC PACKAGING. Manuscript received December 2, 2008; final manuscript received April 22, 2009; published online June 23, 2009. Assoc. Editor: Sandeep Tonapi.

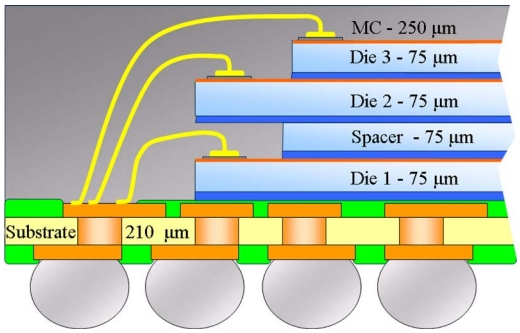

Fig. 1 Typical configuration and dimensions of stacked-die packages

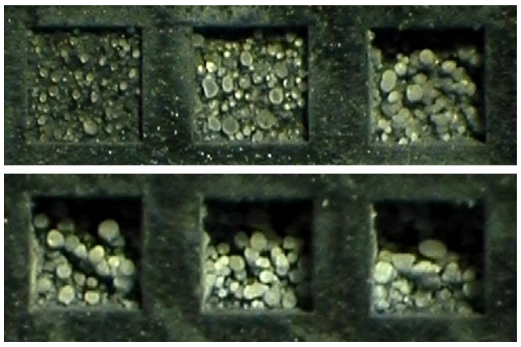

Fig. 2 Optical top view image after five scans with different pulse energies of the femtosecond laser system; boxes size: 0.5×0.5 mm², upper row (left to right): 2.1 μJ, 5 μJ, and 16 μJ, bottom row: 26 μJ, 36 μJ, and 46 μJ

clear which laser source would be best for target preparation in stacked-die packages. Therefore, various laser sources were evaluated experimentally to determine their effects on the material mix of stacked packages.

2 Interaction of Light and Matter

The phenomenon of laser-induced material ablation is a highly complex interaction of several subprocesses, and has been under investigation since the first demonstration of a ruby laser emitting in the infrared optical spectrum in 1960 by Maiman [9].

Ablation is described as a combination of different absorption mechanisms, electronic excitation, rapid heating, ionization, sputtering, melting, vaporization, and ejection [10–12].

A detailed discussion of light absorption in semiconductor material would have to consider seven different absorption mechanisms such as absorption by free electrons, intrinsic and impurity absorption, absorption by lattice oscillations, exciton and plasmon absorption, and finally the intervalence band absorption in silicon and germanium [13].

The development of short-pulse laser sources in the femtosecond range widened the discussion of ablation mechanisms to multiphoton absorption and the development of the two-temperature model for the separate prediction of electron and phonon temperature distributions in metals [14,15].

Nevertheless, the basic interactions of reflection and absorption of a Gaussian beam (a focused coherent laser beam) with the package material have to be discussed, because only the absorbed energy is utilized for the ablation process.

Dielectrics, meaning insulators in the absence of excitation, have electrons only in the valence band without any electrons in the conductive band. These insulating materials are basically transparent, beside nearby the resonance frequency of the oscillator described by the Lorentz model. The classical Lorentz model describes the electron as a harmonic oscillator driven by the oscillating force of the electric field of the optical plane wave. The force exerted by the magnetic field is smaller than that due to the electric field by a factor in the order of v/c (v =electron velocity/c=speed of light) and hence it is usually neglected. Both the classical and the quantum-mechanical treatments yield almost identical expressions for the dielectric function of a nonmetal with only one resonance [16]. In reality, dielectric media contain multiple resonances corresponding to different electronic vibrations. The overall susceptibility arises from superposition of contributions from these resonances [17]. For example, the silica filler of the MC has no resonances between 180 nm and 1400 nm, and is fully transparent in this bandwidth.

For dielectrics, the reflection coefficient is usually below 0.1, meaning the reflection losses are less than 10 percent. In general, reflectivity also depends on the incidence angle and the polarization of a monochromatic plane wave. For laser ablation, laser beams with normal incidence are generally used, so the power reflectance can be described by the Fresnel equations.

Metals have significantly higher absorbance and reflectance. The optical response is dominated by free electron charges in the skin layer. For the theoretical description, the first of the source-free Maxwell equations must be modified by including the current density along with the displacement current density. Since the Maxwell equation takes the same form as the analogous equation for a dielectric medium, the laws of wave propagation are applicable even for conductors [17].

To satisfy the Helmholtz equation, only a complex wavenumber $\tilde{k}$ is necessary, which can be achieved by a complex refraction index $\tilde{n}=n-j\kappa$, where n and $-j\kappa$ denotes the real and the imaginary part, respectively. The imaginary part $-j\kappa$ of the refractive index results in a decrease of the amplitude of the plane wave during propagation in z-direction in the conductive medium, meaning absorption. The insensitivity $I(z)$ decreases with

$$I(z) = I_0 \exp(-2k_0\kappa z) = I_0 \exp(-\alpha z) \tag{1}$$

where $\alpha=2k_0\kappa=\sqrt{2\omega\mu_0\sigma}$ is the conductivity- and wavelength-dependent absorption index with $k_0=2\pi/\lambda$ as the wave number, ω as the frequency of the incident laser beam, μ_0 as the permeability of free space, and σ as the electrical conductivity. In reality, the absorption behavior of metals is more complex because of a number of secondary effects, such as interband transitions, that cause the oscillations in the reflection and absorption spectra. Moreover, the metal atoms also have bound electrons with resonance frequencies in the visible range [18].

The high reflectivity of metals is also caused by the big imaginary part of the refraction index, as mentioned above. The reflectivity coefficients and optical penetration depths for a large number of metals and semiconductor materials for various laser wavelengths were collected by Allmen and Blatter [16]. All metals are highly reflective (97–99%) for infrared laser light, with significant decreases toward shorter wavelengths in the ultraviolet (UV) range. This strong dependence of reflectivity on the laser wavelength has to be considered for the estimation of so-called ablation thresholds. For semiconductor materials, there is a dramatic decrease in the optical penetration depth for wavelengths in the UV range.

3 Results of Laser Evaluation

3.1 Femtosecond Laser Source. A femtosecond laser source with an output wavelength of 1030 nm and a pulse duration of below 500 fs was used for package removal. Pulse energies were varied from 0.5 μJ per pulse up to 52 μJ per pulse; the pulse frequency during all experiments was 10 kHz, resulting in an average output power from 5 mW up to 0.5 W.

With a scan speed of 10 mm/s and a line pitch of 5 μm, all areas were machined with five scans.

The results of MC machining are shown in Fig. 2. The polymer

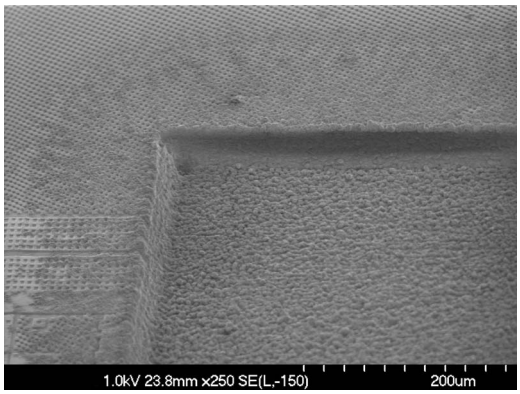

Fig. 3 Scanning electron microscope (SEM) image of an IC surface machined with 16 μJ pulse energy of the femtosecond laser. Surrounding burst particles are up to 150 μm away.

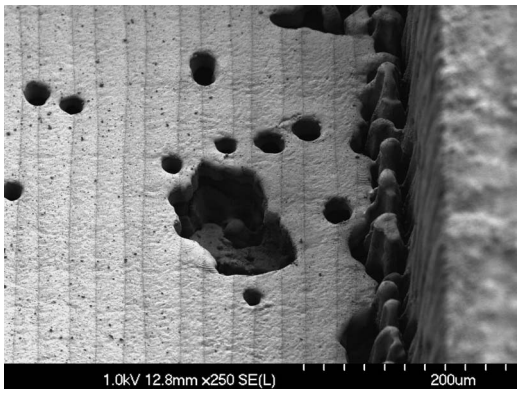

Fig. 4 Silicon die surface after 100 area scans. Pulse energy of the picosecond laser system was 80 μJ; note massive hole occurrence in the bulk silicon.

matrix of the MC was very well ablated by the ultrashort laser pulses. It was remarkable that the silica filler particles remained within the machined area, because they are highly transparent at the infrared laser wavelength. Nearly all filler particles remained at the comparable low energy of 2.1 μJ (Fig. 2). For higher pulse energies, an expulsion of the smaller filler particles occurred, and only more massive particles remained in the machined cavity. Increasing the number of iterations did not improve these results. Therefore, a distinct ablation of standard MC with silica filler particles was not feasible with this femtosecond laser source.

The ablation capabilities for silicon chips were evaluated on a chemically decapsulated IC. Figure 3 shows the results achieved after 20 scans with a pulse energy of 16 μJ. Despite using an optical wavelength in the near infrared range, where silicon is highly transparent, controlled machining of the silicon was possible. Burst particles were observed up to 150 μm away from the machined area.

It was noteworthy that slight variations in the laser settings, e.g., increasing the pulse energy to 21 μJ, created a series of deep holes that are described in more detail below. Further increasing the pulse energy did not result in creation of more or bigger holes.

3.2 Picosecond Laser Source. Picosecond laser sources were evaluated in the infrared and the green light range with an output wavelength of 1030 nm, and a frequency-doubled 515 nm. Pulse lengths were typically 7 ps at a fixed repetition rate of 200 kHz and maximum pulse energies of 250 μJ and 125 μJ, respectively.

Compared with the femtosecond laser source, the distinct removal of MC encapsulation was possible with much better results; filler particles did not remain in the machined area. After six area scans with a pulse energy of 25 μJ, the IC surface was exposed. After eight area scans, neither filler particles nor residue of the polymer matrix were left. They were expelled from the machined area, and thus, did not interfere with the subsequent ablation process.

In order to investigate its feasibility for silicon ablation, the stacked package was machined with various pulse energies from 25 μJ up to 125 μJ per pulse. For both the 1030 nm and the 515 nm ps laser sources, randomly distributed holes of uniform size occurred at all pulse energies, and in some cases, bigger clusters were removed, as shown in Fig. 4.

A mechanical cross section with subsequent ion-polishing through one of the holes is shown in Fig. 5. A hole depth of more than 50 μm and massive tensile cracks by molten and annealed silicon were observed, confirming that the silicon surface was melted by the laser energy. Possibly the deep holes can be explained by phase explosion or explosive boiling within the molten silicon.

3.3 Excimer Laser Source. Excimer lasers are high-pressure gas lasers that emit at a series of discrete wavelengths in the UV range. A compact excimer micromachining system with an output wavelength of 248 nm was evaluated. Pulse duration was 5 ns at repetition rate of 300 Hz and 18 mJ pulse energy. Compared with solid-state laser systems, in excimer laser systems, the machined area is not defined by scanning the laser beam with a galvanometer head. Instead, this excimer laser system has a beam dimension of 6×4 mm^2 that can be shaped by masks. The power density on the sample surface can be varied by demagnifying (expanding) the beam.

The nanosecond UV laser pulses of the excimer laser system were excellent for removing MC, but they created a large heat-affected zone (HAZ) of several hundred micrometers around the machined area, and massive staining of the MC.

Subsequent ablation of the silicon die had unexpected poor results. Ablation of the silicon was not uniform; instead, extreme ejections of molten silicon were observed. A cross section through the center of the machined area is shown in Fig. 6. The deep craters damaged the IC structures down to the fourth engraved die, without removing most of the material of the top silicon dies.

Package cross sections prepared by UV laser sources were described in the literature [19], so these were also evaluated in our study. In general, package cross-sectioning was possible; even the solder balls were machined. However, the detailed view showed massive deposits of molten silicon and molten solder material as well as massive HAZs with vaporized DA tape and die cracking.

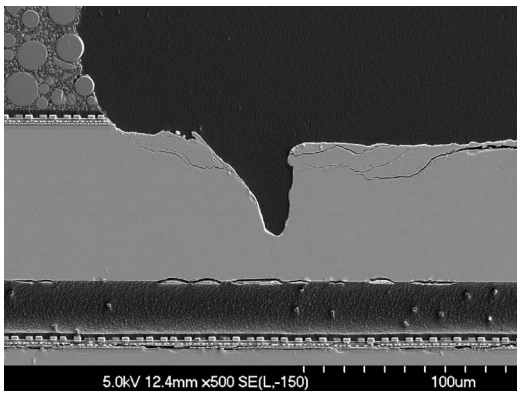

Fig. 5 Mechanical cross section of a hole, probably induced by phase explosion or explosive boiling. Massive tensile cracks by molten and annealed silicon after ten area scans with a pulse energy of 125 μJ can be observed for the picosecond laser system.

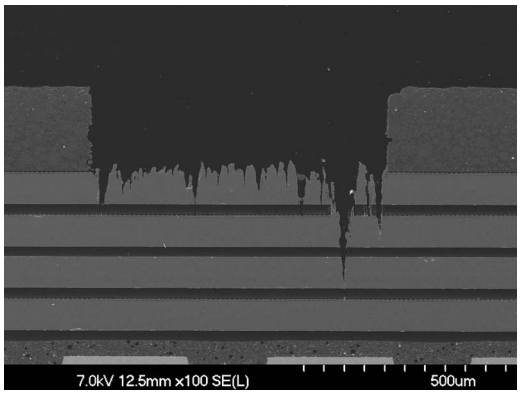

Fig. 6 Mechanical cross section showing deep craters of excimer laser-induced damage in the IC structures down to the fourth engraved die; the material of the top silicon die remains.

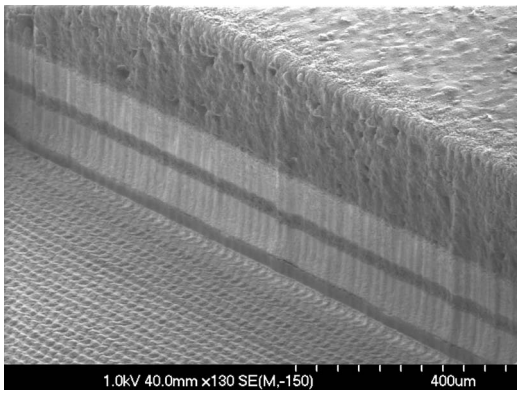

Fig. 8 Tilted view on one edge of the area machined with a 355 nm DPSS laser through the molding compound and the two upper silicon dies (dies 2 and 3)

3.4 Diode-Pumped Solid-State Laser Source. As mentioned previously, infrared DPSS lasers are commonly used for removal of MC, but are not feasible for the machining of silicon dies due to their high transparency. However, the high quality of the beam and the high peak power enable frequency conversion by nonlinear photonic crystals. The second harmonic generation (SHG) or the frequency-trebling third harmonic generation (THG) is used to convert the emitted infrared light to shorter wavelengths in the visible or UV range [20]. Two DPSS lasers with wavelengths at 532 nm and 355 nm, using this principle, were evaluated. Pulse duration was around 6 ns, and the pulse frequency was scaleable from 1 kHz to 200 kHz. The energy per pulse was highly dependent on the pulse frequency. At 20 kHz, the energy amounted to 90 μJ (SHG) and 70 μJ (THG) per pulse, respectively.

The MC removal showed nearly identical results for 1064 nm, 532 nm, and 355 nm pulses. For all wavelengths, the silica filler particles were expelled from the machined area.

The ablation of the silicon dies revealed significant differences in the achieved surface structures for the various laser wavelengths. For the 532 nm wavelength with a pulse frequency of 20 kHz and a scan speed of 450 mm/s, the surface roughness of the silicon increased with the number of laser scans. Figure 7 shows the surface structure of the machined silicon die after 30 laser scans; due to the bigger line pitch of 40 μm, the individual laser rows are visible. Machining the silicon die at 355 nm created a smooth surface. Increasing the number of laser scans did not increase the surface roughness. Reducing the line pitch from 40 μm down to 20 μm resulted in the disappearance of the laser lines and a homogeneous silicon surface that remained homogeneous with an increasing number of scans. The surface roughness of the machined silicon surface was measured in the top and the third die; both had roughnesses of around 5 μm. Figure 8 shows a cross section through the MC and the two upper silicon dies.

The time-effort to perform 160 laser scans was 145 s. An even smoother edge can be achieved by previously removing MC with laser scans in an area, which is a few hundred micrometers larger, to avoid shadowing by silica filler particles.

A mechanical cross section through such a laser edge is presented in Fig. 9, showing the machined MC, DA tape, and the IC structures of the upper two dies. The detailed view shows a relatively small HAZ. Damage is visible only in metal layers located within 4–5 μm of the laser edge. The tension cracks in the upper 500 nm-thick silicon nitride layer occur in this package type on the whole IC surface, also far away from laser edges and in dies without any laser-based target preparation.

4 Summary of Results

Encapsulation removal to get access to the engraved dies is an important factor for laser-based package opening in 3D integrated devices. The main drawback of the femtosecond laser source was its inability to remove MC, due to the remaining silica filler particles in the machined area. The low pulse energy in the μJ range only disrupted the polymer matrix of the MC. Therefore, the femtosecond laser was not the best choice for this application.

Compared with the femtosecond laser source, the picosecond laser sources in the infrared and the green light range were much more effective with respect to well defined removal of MC encapsulation without leaving unacceptable filler particles in the ma-

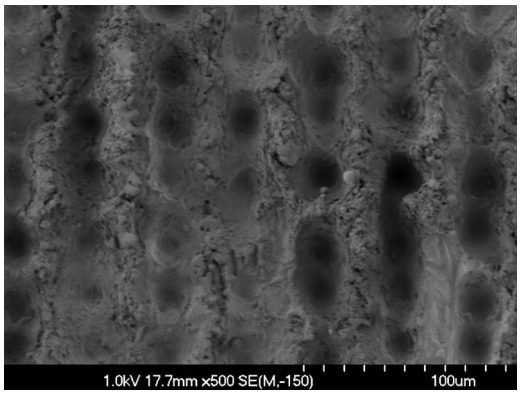

Fig. 7 Top view image of the silicon die after 30 laser scans with 532 nm DPSS laser. With increasing number of scans, the irregularities increase.

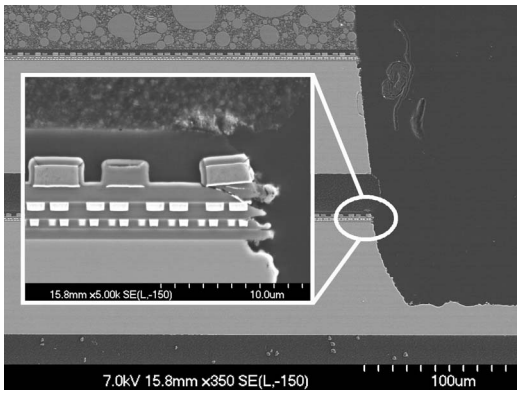

Fig. 9 Mechanical cross section through the laser edge machined with a 355 nm DPSS laser, including detailed view of the cut IC structures with small HAZ

Table 1 Overview and summary of the results for various laser sources and wavelengths for molding compound, silicon, and metals

	Material		
Laser source	MC	Silicon	Cu/Au
Femtosecond laser	−	+	++
Picosecond 1030 nm	+	−	−
Picosecond 515 nm	+	−	+
Excimer 248 nm	++	−	+
DPSS 1064 nm	++	−	−
DPSS 532 nm	++	+	+
DPSS 355 nm	++	++	++

chined area. The excimer laser system we evaluated was very capable of removing MC, but created a large HAZ. DPSS laser systems in the infrared range are state-of-the-art for MC removal, and the DPSS laser systems with shorter wavelengths in the visible or UV range showed the same performance.

The distinct removal of silicon and metal was possible with the femtosecond laser source, even though its wavelength was in the near infrared, where silicon is highly transparent and metals are highly reflective. Our results were consistent with recent publications, describing machining of IC structures with infrared femtosecond laser sources [21]. It was noteworthy that minor variations in the laser settings (e.g., increasing the pulse energy) created a series of deep holes, but a clear trend in the factors involved in hole creation was not discerned.

For both picosecond laser sources at all pulse energies, randomly distributed holes of uniform size were observed in the silicon, and in some cases, bigger clusters were broken out. A cross section through such a hole showed massive tensile cracks by molten silicon, confirming that the silicon surface was melted by the laser energy. One possible explanation for the deep holes is due to phase explosion or explosive boiling within the molten silicon. Detailed studies of this effect were carried out by Doemer [22] with high-speed transmission electron microscopes; highly ionized laser-induced plasma was observed during phase explosion.

With the excimer laser system, the ablation of the silicon die was not feasible for distinct removal of silicon dies. Ablation of the silicon was not uniform; instead, extreme ejections of molten silicon were observed, while most of the material of the top silicon die was not removed.

For DPSS lasers, this study found a significant difference in ablation of silicon dies for 532 nm and 355 nm wavelengths. With the 355 nm DPSS laser, a distinct ablation of the stacked silicon dies was possible with surface roughness of around 5 μm, which also remained after ablation of several silicon dies. Mechanical cross sections through such a laser edge showed a relatively small HAZ with visible damage within 4–5 μm of the laser edge. The removal of MC encapsulation and metals, such as gold wirebond and copper leadframes, is also possible with this laser source. Table 1 summarizes the quality of achieved results for material ablation with various laser sources and wavelengths. The main criterion for MC removal is that the quality of the results must be comparable to the results achieved with state-of-the-art DPSS laser systems in the infrared (IR) range. For the removal of the silicon dies and metals, artifact-free machining with surface roughness in the μm range is the goal.

5 Conclusions and Outlook

The capability for target preparation in highly integrated SiP devices (especially stacked packages) was evaluated for different types of laser sources such as ultrashort-pulse lasers (femtosecond and picosecond), excimer, and DPSS lasers. The influence of pulse duration and emitted wavelength on the specific ablation of stacked packages and large area cross sections is described.

Ultrashort-pulse lasers with pulse durations in the femtosecond range are not suitable for ablation of the MC. For MCs with high filler content, laser pulses with durations in the nanosecond range are the best choice, because during the thermal ablation process, the filler particles are expelled and do not interfere with further ablation.

The picosecond laser sources in the infrared and green light range performed better for MC removal, but also created a series of deep holes in silicon. This is a major drawback for picosecond laser sources.

The excimer laser we evaluated was not capable of distinct removal of silicon dies.

For the removal of stacked silicon dies with DPSS lasers, the laser wavelength is the most important factor. With the UV 355 nm DPSS laser, a distinct ablation of the stacked silicon dies was possible with surface roughness of around 5 μm. Because of the small zone of visible damage in the μm range, this DPSS laser delivered the best results for target preparation in 3D integrated electronic packages.

Estimating the actual propagation of the HAZ with the UV DPSS laser will require more investigation, especially in complete SiP devices with various materials.

Acknowledgment

The authors are indebted to the German BMBF and to the DGE of the French Ministry of Economy, Industry, and Employment, both of which support this work within the project FULL CONTROL. For the support under Grant Nos. 16SV2311 and 062930381 within the EURIPIDES-EUREKA framework, we are very thankful.

References

[1] Winkler, S., 2007, *Advanced IC Packaging*, Electronic Trend, San Jose, CA.
[2] 2008, International Technology Roadmap for Semiconductors (ITRS), SiP White Paper—System Level Integration in the Package, V9.0.
[3] Lee, T. W., 1993, "Mechanical and Chemical Decapsulation," *Microelectronics Failure Analysis, Desk Reference*, 3rd ed., ASM International, Materials Park, OH, pp. 61–74.
[4] Krüger, M., Krinke, J., Ritter, K., Zierle, B., and Weber, M., 2003, "Laser-Assisted Decapsulation of Plastic-Encapsulated Devices," Microelectron. Reliab., **43**, pp. 1827–1832.
[5] Frazier, B. M., Mathews, S. A., Duignan, M. T., Skoglund, L. D., Wang, Z., and Dias, R. C., 2002, "Laser-Based Sample Preparation for Electronic Package Failure Analysis," Proc. SPIE, **4637**, pp. 374–377.
[6] Duebotzky, A., and Krueger, B., 2001, "Evaluation of Alternative Preparation Methods for Failure Analysis at Modern Chip- and Package Technologies," Proceedings of the 27th International Symposium for Testing and Failure Analysis (ISTFA), pp. 83–86.
[7] Hong, M. H., Mai, Z. H., Chen, B. X., Thiam, T., Song, W. D., Lu, Y. F., Soh, C. E., and Chong, T. C., 2002, "Pulsed Laser Ablation of IC Packages for the Device Failure Analysis," Proc. SPIE, **4637**, pp. 445–452.
[8] Carter, G., 2002, "Laser Decapsulation of Transfer Molded Plastic Packages for Failure Analysis," Proceedings of the 28th International Symposium for Testing and Failure Analysis (ISTFA), pp. 117–125.
[9] Maiman, T. H., 1960, "Stimulated Optical Radiation in Ruby," Nature (London), **187**, pp. 493–494.
[10] Li, J., and Ananthasuresh, G. K., 2001, "A Quality Study on the Excimer Laser Micromachining of Electro-Thermal-Compliant Micro Devices," J. Micromech. Microeng., **11**, pp. 38–47.
[11] Marine, W., Bulgakova, N. M., Patrone, L., and Ozerov, I., 2004, "Electronic Mechanism of Ion Expulsion Under UV Nanosecond Laser Excitation of Silicon: Experiment and Modeling," Appl. Phys. A, **79**, pp. 771–774.
[12] Phipps, C. R., 2006, *Laser Ablation and Its Applications*, Springer, New York.
[13] Kirejew, P. S., 1974, *Physik der Halbleiter*, Akademie-Verlag, Berlin.
[14] Wellershoff, S.-S., Hohlfeld, J., Güdde, J., and Matthias, E., 1999, "The Role of Electron-Phonon Coupling in Femtosecond Laser Damage of Metals," Appl. Phys. A, **69**(7), pp. S99–S107.
[15] Rethfeld, B., Kaiser, A., Vicanek, M., and Simon, G., 1998, "Irradiation of Solids With Subpicosecond Laser Pulses: Excitation and Relaxation Dynamics of Electrons and Phonons," Proc. SPIE, **3343**, pp. 388–399.
[16] Allmen, M., and Blatter, A., 1995, *Laser-Beam Interactions With Materials—Physical Principles and Applications*, 2nd ed., Springer, Berlin.
[17] Saleh, B., and Teich, M., 2007, *Fundamentals of Photonics*, 2nd ed., Wiley, Hoboken, NJ.

[18] Reider, G., 2005, *Photonik—Eine Einführung in die Grundlagen*, 2nd ed., Springer, Wien.
[19] Dias, R., Skoglund, L., and Wang, Z., 2002, "Laser Milling Methods for Package Failure Analysis," Proceedings of the 28th International Symposium for Testing and Failure Analysis (ISTFA), pp. 109–115.
[20] Meijer, J., Du, L., Gillner, A., Hoffmann, D., Kovalenko, V. S., Masuzawa, T., Ostendorf, A., Poprawe, R., and Schulz, W., 2002, "Laser Machining by Short and Ultrashort Pulses, State of the Art and New Opportunities in the Age of the Photons," CIRP Ann., **51**(2), pp. 531–550.
[21] Halbwax, M., Sarnet, T., Hermann, J., Delaporte, P., Sentis, M., Fares, L., and Haller, G., 2007, "Micromachining of Semiconductor by Femtosecond Laser for Integrated Circuit Defect Analysis," Appl. Surf. Sci., **254**, pp. 911–915.
[22] Doemer, H., 2004, "Hochgeschwindigkeits-Transmissionselektronenmikroskopie zur Zeitaufgelösten Untersuchung der Laserablation Dünner Metallfolien," Ph.D. thesis, Technische Universität Berlin, Germany.